NanoBiotechnology

ISSN 1551-1286/05/01:327–336/$30.00 (Online) 1551-1294
DOI: 10.1385/Nano:1:4:327

Original Article

Encoded Metal Nanoparticle-Based Molecular Beacons for Multiplexed Detection of DNA

Michael Y. Sha,[1] Mark Yamanaka,[1] Ian D. Walton,[1] Scott M. Norton,[1] Rebecca L. Stoermer,[2] Christine D. Keating,[2] Michael J. Natan,[1] and Sharron G. Penn[1]

[1]Nanoplex Technologies, Inc., 665 Clyde Avenue, Mountain View, CA 94043; and [2]Department of Chemistry, Penn State University, PA

Abstract

In this paper we describe a molecular beacon format assay in which encoded nanowire particles are used to achieve multiplexing. We demonstrate this principle with the detection of five viral pathogens; Hepatitis A virus, Hepatitis C virus, West Nile Virus, Human Immune Deficiency virus and Severe Acute Respiratory Syndrome virus. Oligonucleotides are designed complementary to a target sequence of interest containing a 3′ universal fluorescence dye. A 5′ thiol causes the oligonucleotides to self-assemble onto the metal nanowire. The single-stranded oligonucleotide contains a self-complementary hairpin stem sequence of 10 bases that forces the 3′ fluorophore to come into contact with the metallic nanowire surface, thereby quenching the fluorescence. Upon addition of target DNA, there is hybridization with the complementary oligonucleotides. The resulting DNA hybrid is rigid, unfolds the hairpin structure, and causes the fluorophore to be moved away from the surface such that it is no longer quenched. By using differently encoded nanowires, each conjugated with a different oligonucleotide sequence, multiplexed DNA assays are possible using a single fluorophore, from a multiplexed RT-PCR reaction.

(Nanobiotechnology DOI: 10.1385/Nano:1:4:327)

Key Words: Multiplex; molecular beacon; RNA detection; pathogen; encoded; nanotechnology; nanowire.

Introduction

Molecular beacons *(1)*, which comprise looped DNA structures with fluorophores and quenchers attached to each end of a sequence, have proven extremely valuable for real-time sensing of DNA in solution, including the detection of pathogens *(2)* and single nucleotide polymorphisms *(3)*. In the "dark" state, the loop-induced proximity of the DNA termini lead to fluorescence quenching; the presence of DNA complementary to the loop sequence leads to an extended, "bright" conformation. Multiplexed DNA detection is possible with molecular beacons *(3,4),* but is limited by the number of spectrally distinct fluorophores available, as well as by the need to synchronize the optical properties of the fluorophore and quencher. Encoded substrates used to immobilize molecular beacons for multiplexing have also been reported; however, a quencher is still required in these systems *(5–7)*. Gold nanoparticles, which have novel and tunable optical properties, can serve as quenchers *(8,9)*, and recently this approach has been extended to macroscopic gold surfaces *(10–12)*. However, these approaches do not obviate the need for multiple fluorophores. We describe herein a powerful new approach to multiplexed beacons based on the use of striped, encoded gold and silver nanowires *(13–15)* as quenchers, thereby allowing both

Correspondence and reprint requests to:

Sharron G. Penn,
E-mail: spenn@nanoplextech.com,
Christine D. Keating,
E-mail: keating@chem.psu.edu.

Humana Press

encoding and quenching to be achieved using a nanoparticle This method allows multiplexed DNA assays to be carried out using a single fluorophore without the need for a quencher. In this paper we demonstrate feasibility via the simultaneous detection of five pathogens from a multiplexed RT-PCR reaction. Moreover, the availability of over 1000 different uniquely identifiable striping patterns would allow beacon-based detection of DNA sequences to be extended to arbitrarily high levels of multiplexing, using this nanowire system.

The molecular beacons technology was first described by Tyagi and Kramer in 1996 *(1)*. In this seminal paper the molecular beacon comprised a fluorophore reporter dye and a nonfluorescent quencher chromophore. In close proximity, the fluorophore is quenched by the energy transfer to the nonfluorescent chromophore. Separating the fluorophore and the quencher results in a fluorescent signal. Molecular beacons have been attached to various supports for biosensor applications *(6,16,17)*. For example, Steemers et al. *(6)* demonstrated a fiber optic bead array for parallel detection of three DNA targets, while Wang et al. *(17)* arrayed five molecular beacon probes having various degrees of complementarity to a single target sequence. Tan and co-workers *(16)* have used an array format to optimize surface probe attachment chemistry and other experimental variables.

Metal surfaces can efficiently quench emission from dyes located within a few nanometers of the surface *(18–21)*. Therefore, when molecular beacon probes are attached to metallic surfaces, the surface can provide fluorescence quenching, and no organic quencher dye is required. The presence of metals provides alternative nonradiative energy decay paths that can change the fluorescence quantum yield of a fluorophore. At close distances (<50 Å) fluorescence is quenched and at intermediate distances (75–100 Å), it is enhanced *(19)*. A number of groups have used this phenomenon in a biological assay. Perez-Luna et al. *(12)* have used a gold surface to quench fluorescence of bound molecules and detected emission after displacement in a competitive immunoassay. Others have attached fluorescently labeled oligonucleotides to gold and silver surfaces, to demonstrate proof of principle for nucleic acid assays. Du et al. *(10)* demonstrated quenching of hairpin DNA sequences attached to a planar gold surface, to mimic a microarray experiment, and successfully distinguished two DNA sequences, and more recently expanded this work to investigate the thermodynamic and kinetic response of the sensor *(11)*. Dubretret et al. *(9)* used a hairpin loop beacon probe structure on 1.4 nm gold particles, while Maxwell et al. *(8)* showed that even unstructured oligonucleotide probes could be employed. Fluorescence from the unstructured probes could be quenched because, when oligonucleotides are single stranded, they have flexibility and can form looped structures due to their attraction to the gold surface. In addition, the fluorescent dyes will reversibly absorb onto colloidal silver and gold *(22,23)*. Upon hybridization the double-stranded DNA is rigid such that the fluorescent dye cannot reach the surface.

The major shortcoming of both solution-based and particle-based molecular beacons are the limited multiplexability *(3,4)*. In this paper we report a molecular beacon format assay in which encoded nanowire particles are used to achieve multiplexing. We demonstrate this principle with the detection of five viral pathogens: Hepatitis A virus (HAV), Hepatitis C virus (HCV), West Nile Virus (WNV), Human Immune Deficiency virus (HIV), and Severe Acute Respiratory Syndrome virus (SARS).

Nanobarcodes particles are submicron sized metallic nanowires containing gold and silver segments *(13–15)*. They are fabricated by electroplating inert metals (gold, silver) sequentially into alumina templates. The template is dissolved, leaving behind striped nanowires. The reflectivity of gold and silver is significantly different that when viewed in a microscope with blue illumination (400 nm) the wires appear to be striped. The power of this technology is the ability to generate a library of encoded wires by changing the order of the stripes. The nanowires used in this study were approx 250 nm by 6 μm, and contained six metallic segments. Biomolecules, including nucleic acids and proteins, can be conjugated to the wires, resulting in the capability to perform multiplexed fluorescence-based assays, using a fluorescence microscope for data collection both at 400 nm (reflectivity measurements to define library member) and the optimum fluorescence emission wavelength (to define quantitative assay result).

Materials and Methods

Reagents

Oligonucleotides were purchased from BioSource (Camarillo, CA) and were used as received. We selected the following pathogens, for which non-infectious viral RNA was commercially available (Armored RNA® Technology, Ambion Diagnostics, TX): Severe Acute Respiratory Syndrome (SARS), West Nile Virus (WNV), Hepatitis A (HAV), Hepatitis C (HCV), and Human Immune Deficiency Virus (HIV). All probe and target sequences discussed in this report are detailed in Table 1.

Nanobarcode particles were manufactured as previous described *(13–15)*. Briefly, alternating layers of gold and silver are electroplated into the pores of an alumina template, the template is dissolved using strong base, resulting in the formation of striped nanowires. The nanowires used in this study were 250 nm by 6 μm, and contained six metallic segments. Preliminary data were performed using the following nanowire sequences, where 1 denotes silver and 0 denotes gold. HAV = 001110; HCV = 000111; HIV = 001101; SARS = 101010; WNV = 011001. Later experiments were performed using the following nanowires: HAV = 010110; HCV = 100011; HIV = 010110; SARS = 010011; WNV = 100101.

Molecular Beacon Probe Design

The stem-loop structures of the molecular beacons were designed using MFold software *(24)*. HAV probe sequence was designed from the VP1/VP2 capsid protein interphase

region. The HCV probe sequence was designed from 5′ UTR region. The HIV probe sequence was designed from the gag protein region. The WNV probe sequence was designed from the NS5-2 region. The SARS sequence was designed from the nonstructural polyprotein region.

Probe Attachment Protocols

Oligonucleotide probes were assembled onto the nanowires as follows. Approximately 10^8 nanowires in 100 µL water were washed twice with 10 m*M* PBS, and resuspended in 100 µL 10 m*M* PBS. Next 500 µL of 5 µ*M* oligonucleotide probe was added and allowed to self-assemble overnight at room temperature, with gentle rotation. Following assembly, 600 µL of 0.3 *M* NaCl in 10 m*M* PBS was added, and allowed to react for 2 h. The particles were then washed twice in 0.3 *M* NaCl in 10 m*M* PBS, resuspended in 100 µL 10 m*M* PBS and stored at 4ºC until ready to use.

Hybridization Protocols

Hybridization assays were performed as follows. Approximately 3×10^6 nanowires in 3 µL of PBS, were added to 42 µL of hybridization buffer (HS114, Molecular Research Center, Inc.) target in a volume of 5 µL (for positive control, 5 µL of 10 µ*M* oligonucleotide was used). The target was boiled for 2 min prior to addition to the hybridization buffer. The reaction was tumbled gently for 1 h at 55°C. The nanowires were washed with 500 µL 1X SSC for 5 min, followed by 500 µL 0.1X SSC for 5 min. The particles were resuspended in 50 µL 5 m*M* PBS, and imaged.

RT-PCR and Lambda Exonuclease Digestion

Reactions were performed using the SuperScript one-step RT-PCR kit (Invitrogen, CA). Five microliters viral RNA were incubated at 75ºC for 3 min, and added to a mix containing 25 µL 2X reaction buffer, 1 µL 10 µ*M* primer 1, 1 µL 10 µ*M* primer 2, 1 µL Taq polymerase, and 17 µL H_2O (to 50 µL total reaction volume). Multiplexed RT-PCR was performed using the same reagent concentrations. The following conditions were performed on a thermocycler: 50ºC 30 min, 94ºC 2 min, then 40 cycles at 94ºC 15 s, 60ºC 30 s, and 72ºC 30 s, and a final 72ºC 10 min and hold at 4ºC. The double-stranded PCR product was designed with a 5′ phosphate group, such that lambda exonuclease could be used to digest away the phosphorylated 5′ strand, leaving the non-phosphorylated 3′ strand for hybridization to the MB probe. The reaction was allowed to proceed for 20 min at 37ºC, and then boiled for 1 min to inhibit any further enzyme activity. All PCR products were designed to locate the oligonucleotides complementary sequence approximately in the middle of the amplicon. The lengths of the PCR products were as follows: WNV = 242 bp; HAV = 266 bp; HCV = 410 bp; HIV = 172 bp; and SARS = 190 bp.

Nanowire Probe Surface Coverage Measurements

The probes were dissociated from the nanowires by incubating with β-mercaptoethanol (5 µL) in a high salt buffer (100 µL). The samples were incubated with tumbling overnight and in the dark to minimize bleaching. The following day the reaction mixture was centrifuged at 5000 rpm to pellet the nanowires. The supernatant was collected and fluorescence measurements taken using a fluorimeter. A standard curve using fluorescent oligonucleotides of known concentration was used to determine the concentration of probe released from the nanowiress.

Data Collection and Analysis

Data collection and analysis were performed on a Zeiss Axiovert 100 microscope fitted with a Prior H107 stage, Sutter Instruments 300W Xe lamp with liquid light guide, Physik Instrument 400 micron travel objective Positioner and Photometrics CoolSnapHQ camera. Images were acquired with a 63X, 1.4 NA objective. The microscope and all components were controlled by a proprietary software package (written in-house) that performs intra- and interwell moves, automatically focuses at each new position, acquires a reflectance image of the particles at 405 nm (20 nm band-pass filter), and finally acquires the corresponding fluorescence image with a filter set from Chroma Technology Corporation (HQ 545/30 excitation filter and HQ610/75 collection filter).

The reflectance and fluorescence image pairs were analyzed by NBSee™ Software, a proprietary image analysis software package that identifies the nanowires and quantifies their associated fluorescence. The fluorescence from each nanowire is the mean of the pixels constituting that region of that particle in an image. Typically 25 images are taken in a single well of a microplate. Data analysis of multiplexed assays, which are comprised of multiple nanowire striping patterns for each molecular beacon probe, is done by analyzing the log-mean fluorescence across nanowires of the same striping pattern. For all assays, a single or duplicate well is reserved for ascertaining background fluorescence values for each nanowire striping pattern conjugated to its respective molecular beacon probe. A multiple of this value is subtracted from the log-normal mean fluorescence in each target assay. Error bars in all barplots correspond to confidence intervals at $p = 0.95$ and are representative of interassay error. Specifically, Cox's method *(25)* was used to determine confidence intervals from log-normal fit distributions across histograms of mean-fluorescence intensity of nanowires of the same striping pattern. In the case of duplicate assay wells, the log-normal histogram was generated by combining nanowires of the same striping pattern across duplicate wells.

Results

Figure 1A shows a cartoon representation of the molecular beacon assay, while Fig. 1B shows representative experimental images. The assay works as follows: Oligonucleotides are designed that are complementary to the target sequence, and contain a self-complementary hairpin stem sequence of 10 bases. They are labeled with a universal fluorescence dye at the 3′ end (in this case TAMRA), and a thiol at the 5′ end. The 5′ thiol will cause the oligonucleotides to self-assemble

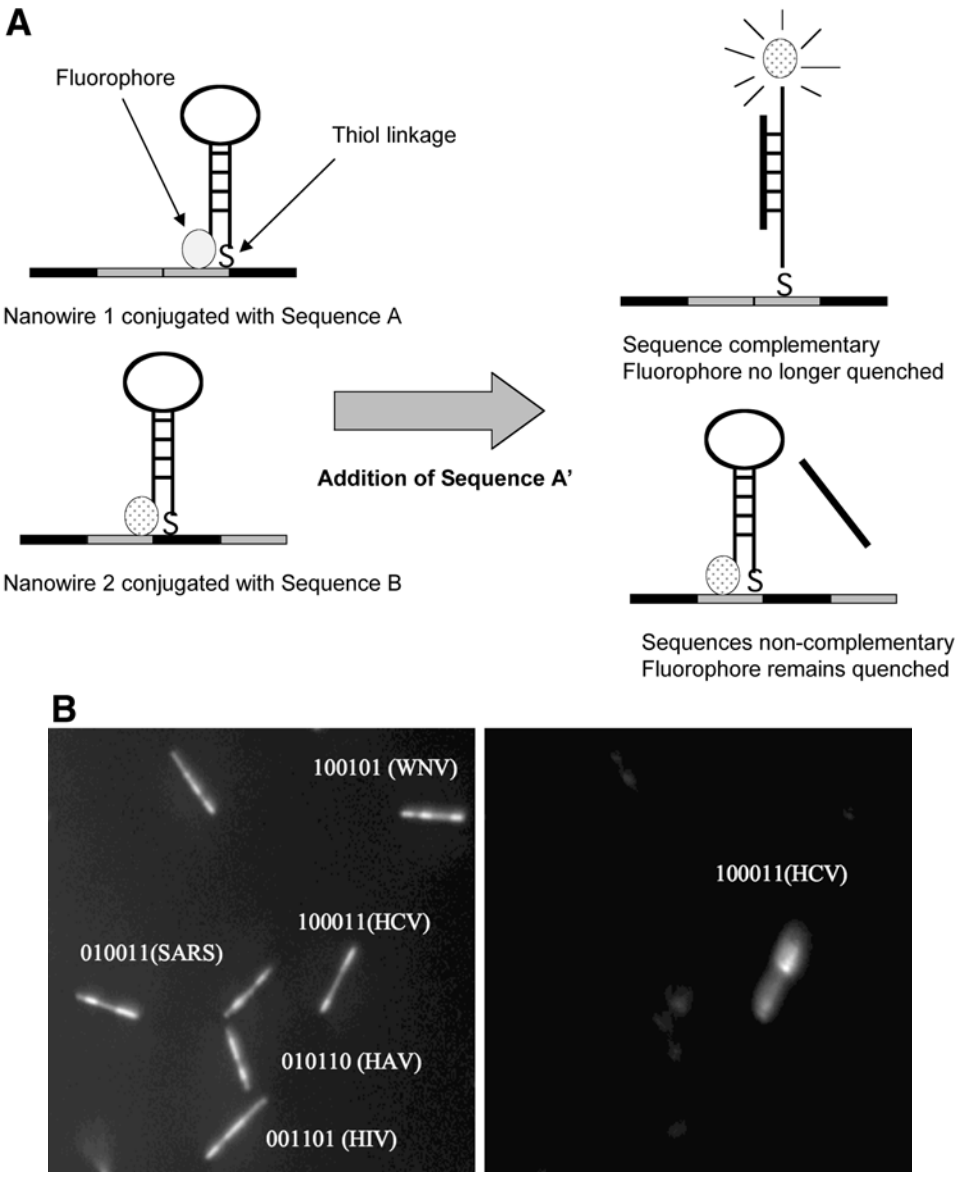

Fig. 1. (A) Cartoon description of assay. Oligonucleotides are designed with a 3′ fluorophore and a 5′ thiol modification. Nanowire library member # 1 is conjugated with oligonucleotide sequence A, via the thiol modification. Nanowire library member # 2 is conjugated with oligonucleotide sequence B, via the thiol modification. The oligonucleotides contain a 10 base hairpin structure, which forces the fluorophore in contact with the metallic nanowire, quenching the dye. Upon addition of target DNA complementary to sequence A, there is hybridization with the complementary oligonucleotides conjugated to nanowire library member # 1. The resulting DNA hybrid causes the fluorophore to be moved away from the surface, such that it is no longer quenched. Upon analysis with a fluorescence microscope, nanowire library member # 1 appears fluorescent and nanowire library member # 2 is not. **(B)** Representative experimental image. Left image = reflectance image showing five populations of nanowires, each conjugated to a different oligonucleotides as indicated. Populations can be ascertained by the different striping patterns seen on the wires. Right image = fluorescence image. Upon addition of HCV oligonucleotides target only nanowire 10011 gives fluorescence signal. All other striping patterns of nanowires do not give fluorescence signal.

onto the metal nanowire. Each nanowire library member is functionalized with a different oligonucleotide sequence. The single-stranded oligonucleotide contains a hairpin stem sequence that forces the 3′ fluorophore to come into contact with the metallic nanowire surface, thereby quenching the fluorescence. Upon addition of target DNA, there is hybridization with the complementary oligonucleotides. The resulting DNA hybrid is rigid, unfolds the hairpin structure, and causes the fluorophore to be moved away from the surface such that it is no longer quenched. Upon analysis with a fluorescence microscope one nanowire library member will appear fluorescent and the other nanowire will be dark. Decoding of the nanowire striping pattern indicates which DNA sequence was present.

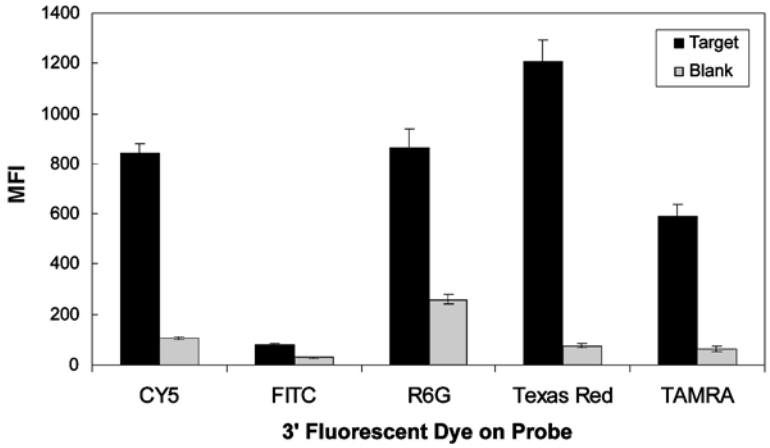

MFI	Cy5	FITC	R6G	Texas Red	TAMRA
Target	842.6	81.0	865.5	1206.8	587.8
No Target	106.1	30.7	259.7	76.8	65.2
% quenching	87 %	62 %	70 %	94 %	89 %

Fig. 2. Comparison of quenching efficiencies of fluorescence dyes as molecular beacons. Oligonucleotide probe sequence HCV was synthesized with five different 3′ fluorophores: Cy5, FITC, Rhodamine 6G (RG6), Texas Red, and TAMRA. Each oligonucleotide was conjugated to nanowire sequence 000111 (0 = gold, 1 = silver). Fully complementary target sequence HCV-T was added at a concentration of 1 μ*M* (50 pmol in 50 μL reaction), and hybridization experiments were performed as described in the Methods section. The experiment was performed in duplicate, and the quenching efficiency determined for each dye. Error bars indicate 95 % standard error across all particles in duplicate experiments. Quenching efficiency is calculated as [1 – (signal from negative control/signal with added target)]%, and actual values from the graph are shown in the table. MFI = mean fluorescence intensity (arbitrary units).

While this assay is conceptually straightforward and elegant, a number of fundamental measurements were required to determine the optimum design for the assay. Preliminary results into the investigation of thiol position on the probe indicated that 5′ thiol gave superior results over a 3′ thiol. We believe this may be due to the higher purity of 5′ thiol oligonucleotides, because they are easier to synthesize. In addition, during the course of these experiments we chose to work with nanowires containing similar amounts of gold and silver; however, experiments showed minimal difference in the quenching with different striped particles (results not shown). All oligonucleotides sequences discussed in the text are given in Table 1.

The choice of fluorescence dye in any molecular beacon–based experiment can have a large impact on the attainable results. The challenge for this system was to find a dye that had ideal quenching properties, but without interfering with the determination of the striping pattern when taking reflectivity measurements at 400 nm. Because differences in the affinity of various dyes to the metal surface or in the fluorescence excitation/emission wavelengths or lifetime might be expected to impact performance in these assays, we performed experiments to determine the optimum organic fluorescent dye. We designed an oligonucleotide sequence complementary to the HCV 5′ UTR region, and varied the 3′ fluorophore, using Cy5, FITC, Texas Red, Rhodamine 6G (R6G), and TAMRA. Complementary target oligonucleotides was added to determine the quenching efficiency, and the results are shown in Fig. 2. Quenching efficiency is calculated as (1 – [signal from negative control/signal with added target]) %. FITC and R6G had the poorest quenching efficiency at 62% and 72%, respectively. Cy5 had a quenching efficiency of 87%, Texas Red had a quenching efficiency of 94%, and TAMRA had a quenching efficiency of 89%. Dubretret et al. *(9)* reported quenching efficiencies for FITC, R6G, Texas Red, and Cy5 when using 1.4 nm gold nanoparticles, which all quenched with greater than 98% efficiency. We postulate that the slight quenching efficiency differences between our results and those of Dubretret et al. *(9)* are due to the nanowires being more representative of a planar surface, such that steric hindrance is likely a greater issue than on small (1.4 nm) spherical nanoparticles. In addition, we are using a fluorescence microscope with filters to collect data (rather than a spectrometer), such that any shift in wavelengths of absorbance or emission would impact our data, compared to data collected using a fluorimeter. While both Texas Red and TAMRA gave good results in the nanowire experiments, we selected TAMRA as the candidate for all subsequent experiments due to commercial availability.

The effect of probe and target length on assay performance was investigated, because it is well documented that the quenching phenomenon is distance dependent *(19)*, and the results are shown in Fig. 3. Three probes were designed to

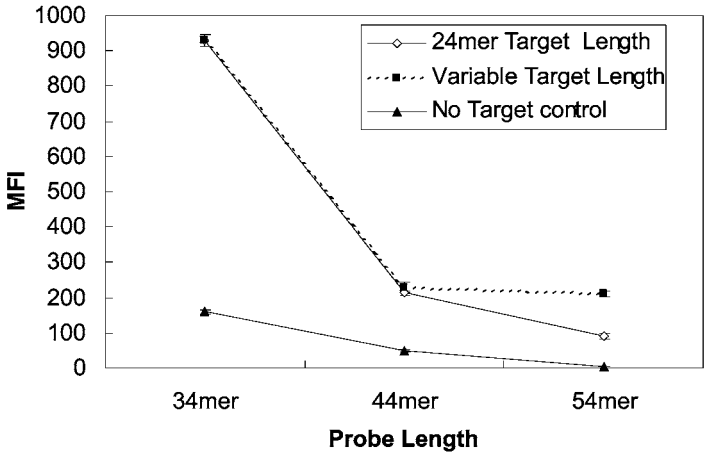

Fig. 3. Effect of probe and target length on assay performance. Three oligonucleotide probes were designed, of 34 (HCV), 44 (HCV-44mer), and 54 (HCV-54mer), bases in length, containing a common 10 base "stem" sequence such that the HCV sequences composed 24, 34, and 44 bases of the entire probe sequences. Three corresponding target oligonucleotides were designed, which were 24 (HCV-T), 34 (HCV-44mer-T) and 44 (HCV-54mer-T) bases in length and were complete matches to the three probe sequences. Error bars represent 95% standard error of all nanowires across two experiments. Open diamonds represent signal for each of the three different probe lengths, each hybridized with the 24mer target (HCV-T). Filled squares represent signal for each of the three different probe lengths, hybridized with corresponding target lengths (HCV with HCV-T; HCV-44mer with HCV-44mer-T; HCV-54mer with HCV-54mer-T). Filled triangles represent negative control, with no added target oligonucleotides. MFI = mean fluorescence intensity (arbitrary units).

the HCV 5′ UTR region, which were 34, 44, and 54 bases in length. They each contained a common 10 base "stem" sequence such that the pathogen sequence composed 24, 34, and 44 bases of the entire probe sequences. Three corresponding target oligonucleotides were designed that were 24, 34, and 44 bases in length and were complete matches to the three oligonucleotide probes (but did not contain the 10 base stem sequence). In Fig. 3, open diamonds represent signal from experiments in which each of the three different length probe sequences were hybridized with the 24mer target sequence. The filled triangles represent signal from the negative controls, in which no target was added. The results show that, under the assembly conditions used for this experiment, the shortest probe (34mer) gave the greatest signal and discrimination between on and off. To rule out the possibility that the target length and not the probe length was a factor in the quenching efficiency, an assay was performed in which the probe and target lengths were equal. These data are represented in Fig. 3 by filled square symbols. In this experiment 34mer probe was hybridized with 24mer target, 44mer probe was hybridized with 34mer target, and 54mer probe was hybridized with 44mer target. Again, the shortest probe:target combination was found to give the best discrimination between on and off. Note that all probes were attached under identical conditions; therefore, while we anticipate some differences in probe surface density and hybridization efficiency between these samples based on steric considerations *(26)*, the trend indicates that the shortest probe:target combination gives the best discrimination. Interestingly the shortest probe:target comination also gave the largest signal, possibly due to the ability of the longer hybrids being able to interact with the surface in some manner. It is also important to note that it is likely both probe length and probe secondary structure play a part in the data. All subsequent experiments were performed with 34mer probes (of which the 10 base stem was included in the 34 bases).

In order to fully characterize the system, we determined the surface coverage of probes on the nanowires, when assembled under the conditions described in the paper. Using the HIV probe, we determined that 3.4×10^{-12} moles of fluorescent oligonucleotides were bound to a population of 50,000,000 nanowires. Assuming the surface area of a nanowire to be 6 μm^2, we calculated a surface coverage on the order of 40,000 oligonucleotides per nanowire (7×10^{-11} oligos/cm^2). For the data described in this paper, approx 2–3 million nanowires were used in each experiment, and images containing 100–200 nanowires of each library member were analyzed.

To demonstrate proof of principle for a *multiplexed* molecular beacon bioassay, we performed a 5-plex experiment using oligonucleotide targets. Five oligonucleotide probes were designed complementary to the genomes of HIV, SARS, WNV, HAV, and HCV. Each probe was 34–36 bases in length, and contained a common 10 base hairpin sequence (see Table 1 for sequences). Each probe was conjugated to a different nanowire library member and the nanowires were pooled. Experiments were performed in which each of the targets were added individually, all five targets were pooled and added simultaneously, and control experiments in which non-complementary target and a "no target" control were performed. The targets were added at a concentration of 1 μM. The results (Fig. 4) show that each target is easily detected in the five nanowire experiment,

Table 1
List of All Sequences Used in Manuscript

Classification	Name	Sequence	Tm
Probe	HCV	5' thiol (CH2)6 gcgag CAT AGT GGT CTG CGG AAC CGG TGA ctcgc (CH2)7 TAMRA -3'	80
Target	HCV-T	TCA CCG GTT CCG CAG ACC ACT ATG	80
Probe	HCV-44mer	5' thiol (CH2)6 gcgag CAT AGT GGT CTG CGG AAC CGG TGA GTA CAC CGG A ctcgc (CH2)7 TAMRA -3'	87
Probe	HCV-54mer	5' thiol (CH2)6 gcgag CAT AGT GGT CTG CGG AAC CGG TGA GTA CAC CGG AAT TGC CAG GA ctcgc (CH2)7 TAMRA -3'	89
Target	HCV-44mer-T	TCC GGT GTA CTC ACC GGT TCC GCA GAC CAC TAT G	87
Target	HCV-54mer-T	TCC TGG CAA TTC CGG TGT ACT CAC CGG TTC CGC AGA CCA CTA TG	90
Probe	HCV-Flu	5' thiol (CH2)6 gcgag CAT AGT GGT CTG CGG AAC CGG TGA ctcgc (CH2)7 fluorescein -3'	80
Probe	HCV-R6G	5' thiol (CH2)6 gcgag CAT AGT GGT CTG CGG AAC CGG TGA ctcgc (CH2)7 Rhodamine 6G -3'	80
Probe	HCV-red	5' thiol (CH2)6 gcgag CAT AGT GGT CTG CGG AAC CGG TGA ctcgc (CH2)7 Texas red -3'	80
Probe	HCV-Cy5	5' thiol (CH2)6 gcgag CAT AGT GGT CTG CGG AAC CGG TGA ctcgc (CH2)7 Cy5 -3'	80
Probe	WNV	5' thiol (CH2)6 gcgag TGT GAA TTG GGT CCC TAC CGG AAG AA ctcgc (CH2)7 TAMRA -3'	79
Target	WNV-T	TTC TTC CGG TAG GGA CCC AAT TCA CA	79
Probe	HIV	5' thiol (CH2)6 gcgag ACC ATC AAT GAG GAA GCT GCA GAA TGC TCG C (CH2)7 TAMRA -3'	77
Target	HIV-T	CAT TCT GCA GCT TCC TCA TTG ATG GT	77
Probe	SARS	5' thiol (CH2)6 gcgag AGA TGC TGT GGG TAC TAA CCT ACC T ctcgc (CH2)7 TAMRA -3'	77
Target	SARS-T	AGG TAG GTT AGT ACC CAC AGC ATCT	77
Probe	HAV	5' thiol (CH2)6 gcgag GAC TGA CTT CTC CTT CTA ATA AT ctcgc (CH2)7 TAMRA -3'	70
Target	HAV-T	ATT ATT AGA AGG AGA AGT CAG TC	70
RT-PCR primer	HCV 5p	5' phosphate TAG TAT GAG TGT CGT GCA GC 3'	73
RT-PCR primer	HCV3'	5' GTC GTC CTG GCA ATT CCG 3'	74
RT-PCR primer	HIV 5p	5' phosphate AGT GGG GGG ACA TCA AGC AGC CAT GC	83
RT-PCR primer	HIV 3'	GAC TGG ATG CAA TCT ATC CCA TTC TGC AGC	82
RT-PCR primer	SARS 5p	5' phosphate GAA GCT ATT CGT CAC GTT CG	73
RT-PCR primer	SARS 3p	CTG TAG AAA ATC CTA GCT GGA G	73
RT-PCR primer	WNV 5p	5' phosphate AGA GAC CTG CGG CTC ATG	75
RT-PCR primer	WNV 3'	AAC ATG TCC TCT GTT GTC ATC CA	73
RT-PCR primer	HAV 5p	5' phosphate ATT GGA AAA CTT ATT GTG TAC TGT TA	70
RT-PCR primer	HAV 3'	TGT GGT AAC ATC CAT AGC AT	69

Lower-case bases indicate hairpin sequence.

when added individually and when the five targets are pooled and added together. The slight differences in intensities between different targets is most likely due to subtle differences in hybridization efficiency between the different probes due to sequence differences.

Following proof of principle work with oligonucleotide targets, we progressed to "real-world samples." We purchased cloned, sequence-defined pathogen RNA (Armored RNA® Technology products, Ambion Diagnostics, TX). It should be noted that by using the Armored RNA products, we were limited to 172–410 base pairs of sequence (depending on pathogen) in which to design PCR primers and probes, which limited the ability to optimize both PCR and probe sequences effectively. Following RT-PCR amplification, we compared double- and single-stranded PCR products in a single plex format. Single-stranded PCR material was generated by incorporating a phosphate on the 5′ end of the 5′ PCR primer and using lambda exonuclease to digest away the phosphorylated 5′ strand, leaving the nonphosphorylated 3′ strand for hybridization to the sequence specific oligonucleotide probe. Results (not shown) indicated that single-stranded PCR product gave better sensitivity.

Reaction conditions were developed for a 5-plex RT-PCR reaction (*see* Materials and Methods section), which amplified

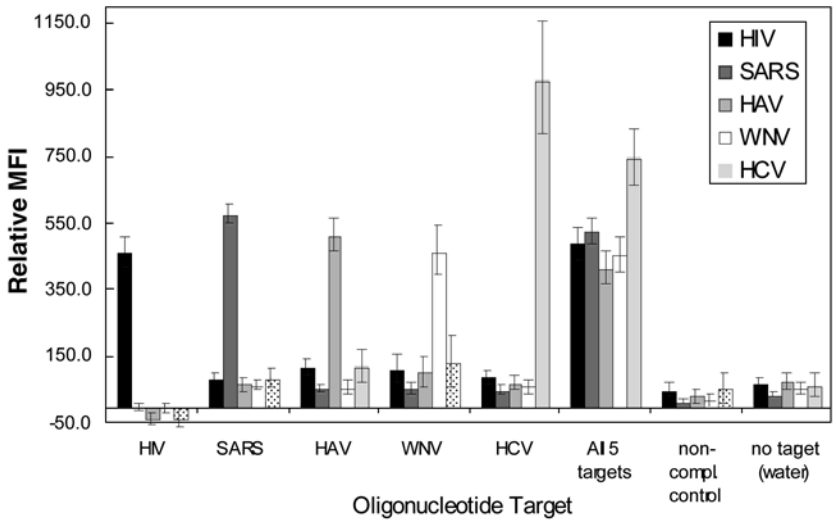

Fig. 4. A 5-plex assay using oligonucleotide targets. The experiment was performed in triplicate, and the signals from the noncomplementary target negative control was used to perform a background subtraction. Error bars indicate 95% standard error across all particles. MFI = mean fluorescence intensity (arbitrary units).

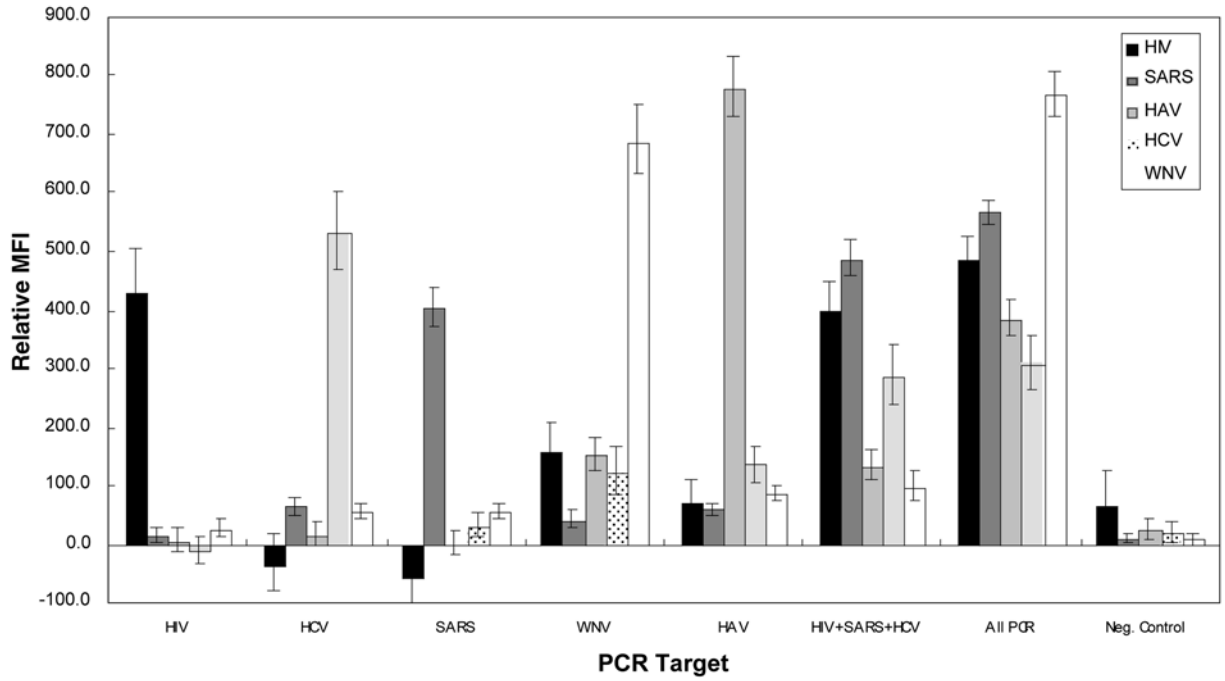

Fig. 5. A 5-plex assay using RT-PCR products. The experiment was performed in duplicate, and the signals from the noncomplementary target negative control was used to perform a background subtraction. Error bars indicate 95% standard error across all particles. MFI = mean fluorescence intensity (arbitrary units).

material from all five RNA products simultaneously. Five nanowire library members were conjugated with the molecular beacon sequences for HAV, HCV, HIV, SARS, and WNV. As before, each probe was conjugated to a different nanowire library member and the nanowires were pooled. Amplification experiments were performed in which each of the five viral RNAs was introduced to a different amplification reaction (each containing all 10 PCR primers), an experiment in which three of the five RNAs were added to the amplification reaction, and an experiment in which all five RNAs were added. Following digestion to obtain single stranded product, each of the reaction products was used to perform a nanowire assay and the results are shown in Fig. 5. The results show that excellent discrimination is seen, and signal to noise ratios

when using RT-PCR amplification products are similar to the use of clean oligonucleotides targets. This is an excellent result, especially given the sequence constraints imposed by working with small cloned RNA products as starting material. A negative control, using single-stranded DNA of the human P450 gene sequence in the PCR reaction, showed very low background signal.

We have demonstrated proof of principle for a novel, multiplexed, pathogen detection assay that combines the use of a metal-encoded nanoparticle, with the spectroscopic phenomenon that metallic surfaces quench fluorescence. This is a new approach to the use of molecular beacons, which allows one to attain much greater multiplexing than currently achievable, and obviates the need for a quencher moiety. This assay offers high selectivity due to the leveraging of DNA secondary structure, and requires no instrumentation beyond a fluorescence microscope that is already present in many laboratories and first responder units. We have applied this approach to the simultaneous detection of five pathogens; HAV, HCV, WNV, HIV, and SARS, from a multiplexed RT-PCR reaction. It should be noted that this assay can be adapted to a plate format for use in a high-throughput setting. The ability to multiplex beyond the 5-plex assay presented in this paper is attainable; we have recently completed the synthesis of a 1000-member nanowire library. In addition, work continues on this assay format, to improve sensitivity and specificity and to increase multiplexing. While we demonstrate a viral RNA analysis application in this paper, this assay should also be applicable to many other DNA analysis assays including SNP detection, gene expression, bacterial biothreat agent detection, mutation detection, and resequencing.

Acknowledgments

Authors thank Gabriela Chakarova and Frances Wong for nanowire synthesis. Work at Nanoplex Technologies Inc. was funded by the National Science Foundation, through an SBIR Phase 1 grant (0418748), and by the National Institute of Standards and Technology (Grant 70NANB1H3028). Work at Penn State University was funded by the National Institutes of Health (RO1 EB00268). CDK also acknowledges support from a Beckman Foundation Young Investigator Award and a Sloan Fellowship.

References

1. Tyagi, S. and Kramer, F. R. (1996), *Nat. Biotechnol.* **14,** 303–308.
2. Vet, J. A. M., et al. (1999), *Proc. Natl. Acad. Sci. USA* **96,** 6394–6399.
3. Marras, S. A. E., Kramer, F. R., and Tyagi, S. (1999), *Genet. Anal. -Biomol. Eng.* **14,** 151–156.
4. Varma-Basil, M., et al. (2004), *Clin. Chem.* **50,** 1060–1062.
5. Horejsh, D., et al. (2005), *Nucleic Acids Res.* **33,** e13.
6. Steemers, F. J., Ferguson, J. A., and Walt, D. A. (2000), *Nature Biotechnol.* **18,** 91–94.
7. Wang, H., et al. (2002), *Nucleic Acids Res.* **30,** e61.
8. Maxwell, D. J., Taylor, J. R., and Nie, S. (2002), *J. Am. Chem. Soc.* **124,** 9606–9612.
9. Dubertret, B., Calame, M., and Libchaber, A. J. (2001), *Nat. Biotechnol.* **19,** 365–370.
10. Du, H., Disney, M., Miller, B., and Krauss, T. (2003), *J. Am. Chem. Soc.* **125,** 4012, 4013.
11. Du, H., Strohsahl, C. M., Camera, J., Miller, B., and Krauss,T. (2005), *J. Am. Chem. Soc.* **127,** 7932–7940.
12. Perez-Luna, V. H., et al. (2002), *Biosens. Bioelectron.* **17,** 71–78.
13. Nicewarner-Pena, S. R., et al. (2001), *Science* **294,** 137–141.
14. Reiss, B. D., et al. (2002), *J. Electranal. Chem.* **522,** 95–103.
15. Walton, I. D., et al. (2002), *Anal. Chem.* **74,** 2240–2247.
16. Yao, G. and Tan, W. (2004), *Anal. Biochem.* **331,** 216–223.
17. Wang, H., et al. (2002), *Nucleic Acids Res.* **2002,** e61.
18. Enderlein, J. (2000), *Biophys. J.* **78,** 2151–2158.
19. Lakowicz, J. R. (2001), *Anal. Biochem.* **298,** 1–24.
20. Moskovits, M. (1985), *Rev. Mod. Phys.* **57,** 783–826.
21. Wokaun, A., Lutz, H. -P., King, A. P., Wild, U. P., and Ernst, R. R. (1983), *J. Chem. Phys.* **79,** 509–514.
22. Nie, S. and Emory, S. R. (1997), *Science* **275,** 1102.
23. Krug, J. T., II, Wang, G. D., Emory, S. R., and Nie, S. (1999), *J. Am. Chem. Soc.* **121,** 9208–9214.
24. Zucker, M. MFold shareware (2003), http://www.bioinfo.rpi.edu/applications/mfold/.
25. Zhou, Xiao-Hua, and Gao, S. (1997), *Stat. Med.* **16,** 783–790.
26. Nicewarner-Pena, S. R., Raina, S., Goodrich, G. P., Fedoroff, N. V., and Keating, C. D. (2001), *J. Am. Chem. Soc.* **124,** 7314–7323.